

WATER ICE/FROST DEPOSITION AT LOW LATITUDES ON MARS: THERMAL MODELING PREDICTIONS.

F.G. Carozzo¹, G. Bellucci¹, F. Altieri¹, E. D'Aversa¹, ¹INAF, Istituto di Fisica dello Spazio Interplanetario, via del Fosso del Cavaliere, 100 – 00133 Rome, Italy; (giacomo.carozzo@ifsi-roma.inaf.it)

Introduction: The main reservoirs of water ice on Mars are in the north polar cap, the south polar cap deposits [1,2,3], the clouds in the form of water ice crystals [4], and at high latitudes in the form of frost and ice [5]. Indirect measurements of the surface/subsurface ice distribution have been carried out by the GRS instrument [6,7]. Water ice is probably responsible of various landforms observed on Mars at equatorial-tropical latitudes [8,9,10]. Its presence could be very important not only from the geological point of view but also from an exobiological perspective. We are using the data of the OMEGA mapping spectrometer to investigate the presence and evolution of frost/ice at low latitudes [11, work in progress]. In this paper we report on the results of a thermal model which we have used to predict the deposition of water frost/ice in the regions identified so far.

Results: The water frost/ice is found on the slopes, along the walls of numerous craters, scarps and feet of hills between 15°S-30°S, in fall/winter, and 15°N-30°N, in summer.

Water frost/ice is located in the shadow regions on the slopes. This shows a clear relationship with the local illumination conditions which favors the deposition of water frost/ice on the surface when the temperatures are very low. In order to verify this, we have implemented a thermal model, including the effect of the illumination on the slopes. We have followed a scheme similar to that adopted by previous workers [12,13] by solving the heat transfer equation for surface temperature and adopting the appropriate boundary and initial conditions. We do not take into account water vapor transport/diffusion in and from the subsurface and we assume a constant composition with depth. We refer to these papers for a detailed description of the thermal model.

In this paper we only refer to the thermal model of the southern hemisphere.

Southern hemisphere: we only plot the results of the models for two extreme cases: the less favorable one, case 1 (latitude=15°S, A=0.14, I=244 J·m⁻²·k⁻¹·s^{-1/2}) and the most favorable one, case 2 (latitude=30°S, A=0.24, I=244 J·m⁻²·k⁻¹·s^{-1/2}), for the frost/ice deposition on the surface. For the case 1 the water vapor is the mean along all the longitude at 15°S, while for the case 2 the water vapor is the mean along all the longitude at 30°S. The water vapor abundance is taken from MCD (Mars Climate Database) [14,15]. The mean thermal inertia in this range of latitudes is ~244 J·m⁻²·k⁻¹·s^{-1/2}. Thermal

inertia data have been taken from TES [16]. We fix two values for the bolometric albedo because at these latitudes there are two type of terrains with different albedo, the first with low-medium albedo and the second with medium-high one. The mean bolometric albedo for those low-medium is ~0.14, while for those medium-high albedo is ~0.24 [17].

We assume that water ice/frost can deposits on the surface when the atmosphere is saturated all the day. Figures 1a (case 1) and 1b (case 2) show the results of thermal modeling for surfaces on different pole-facing slopes (5°,10°,15°,20°,25°) in each case. The grey region on the plots indicates the saturation regime, while the white region the no-saturation regime. Black points are the OMEGA observations, while those red are the OMEGA observations where the frost/ice is found. Blue curve is the mean annual evolution of water vapor, while red ones is the mean annual evolution of minimum and maximum temperature.

For case 1, whole day saturation never occurs. The saturation regime only occurs during the night and early in the morning.

In case 2, the atmosphere becomes saturated the whole day as soon as the slope is increased up to 20° during the end of the fall and early in the winter. For a slope of 25° the atmosphere is saturated during all day for Ls between ~55° and ~120°. Decreasing the slope at 20° we got whole day saturation in a smaller period (80°÷100°). In the remaining cases the saturation never occurs in the middle of the day.

As it seen in figure 1b, fixing the thermal inertia at 244 J·m⁻²·k⁻¹·s^{-1/2}, some OMEGA observations where the frost/ice is found (red points) are in a no-saturation regime. This is an apparent contrast with the result of thermal model. However, given a certain local time, the model has not a memory of what is occurred during the previous hours or previous Ls and therefore it does not consider the increase of thermal inertia caused by the formation of ice. In fact, the presence of ice can change the thermal conductivity, heat capacity, and density of soil and consequently thermal inertia can increase [18]. Using the same approach of Shorghofer and Aharonson [18] we get I~2100 J·m⁻²·k⁻¹·s^{-1/2} for ice/dust mixed soil. This value has been obtained with following assumptions. For a dry soil we assume a porosity of 0.4, a thermal inertia of 150 J·m⁻²·K⁻¹·s^{-1/2}, a heat capacity of 800 J·kg⁻¹·K⁻¹ [19] and a soil density of 3474·kg·m⁻³ derived by the relation of Mellon and Jakosky [20]. While for the ice the thermal properties are: heat capacity=1540 J·kg⁻¹·K⁻¹, ice density=927 kg·m⁻³ and ice

conductivity=3.2 W·m⁻²·K⁻¹ [19]. If we consider a dust/ice mixed with the thermal inertia above mentioned, the latitude and the albedo of case 2, all the OMEGA observations with water frost/ice fall inside the saturation regime beginning from slope of 10° (figure 1c, case 3). In conclusion, the model is able to justify the presence of superficial frost/ice identified by OMEGA only if we assume an increase of thermal inertia due to the ice formation. Because of the thermal model we applied does not take into account the sublimation/deposition rate, we are not able to discriminate if OMEGA is observing ice formation cyclically during the day, or ice stable beginning from the winter solstice up to Ls=150°.

References: [1] Titus et al. (2003) *Science*, 299, 1048-1051. [2] Bibring et al. (2004) *Nature*, 428, 627-630. [3] Langevin et al. (2005) *Science*, 307, 1584-1586. [4]

Curran et al. (1973) *Science*, 182, 381-383. [5] Jones et al. (1979) *Science*, 204, 799-806. [6] Feldman et al (2002) *Science*, 297, 75-78. [7] Boynton et al. (2002) *Science*, 297, 81-85. [8] Neukum et al. (2004) *Nature*, 432, 971-979. [9] Head et al. (2005) *Nature*, 434, 346-351. [10] Milkovich et al., (2006) *Icarus*, 181, 388-407. [11] Carrozzo et al. (2007) *LPSC XXXVIII*, abstract #2096. [12] Aharonson and Schorghofer, (2006) *JGR*, 111, E11007. [13] Schorghofer and Edgett (2006) *Icarus*, 180, 321-334. [14] Lewis et al. (1999) *JGR*, 104, E10,24177-24194. [15] Forget et al. (2007) *Seventh ICM*, abstract #1353. [16] Putzig et al. (2005) *Icarus*, 173, 325-341. [17] Christensen et al. (2001) *JGR*, 106, 23,823-23,872. [18] Shorghofer and Aharonson (2005) *JGR*, 110, E05003. [19] Lide (Ed.) (2003) *CRC Handbook of Chemistry of Physics, 84th ed., CRC Press, Boca Raton, Fla.* [20] Mellon and Jakosky (1993) *JGR*, 98, E2, 3345-3364.

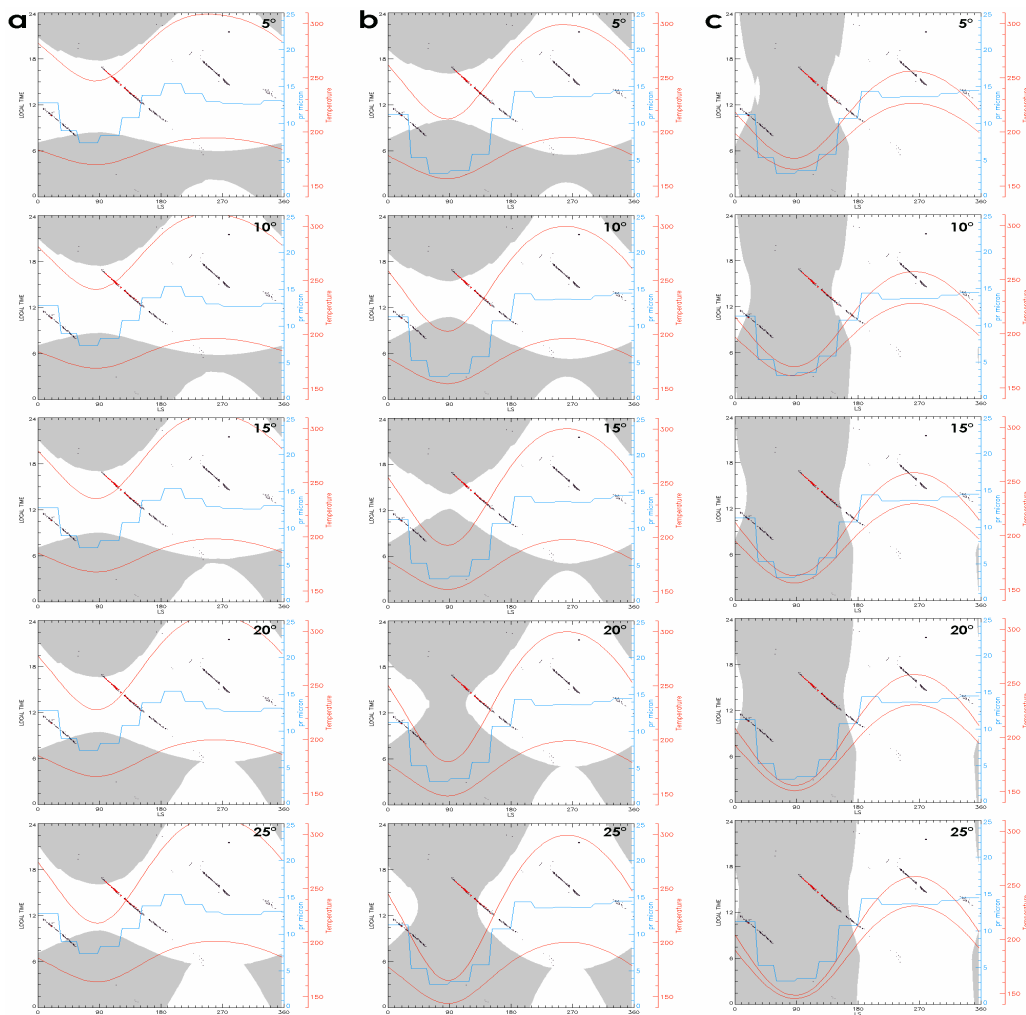


Figure 1. Results of thermal modelling for surfaces on different pole-facing slopes (5°, 10°, 15°, 20°, 25°) for case 1 (fig. 1a), case 2 (fig. 1b) and case 3 (fig. 1c). Solar Longitude (Ls) as a function of local time. In grey is indicated the water vapor saturation region, while in white the water vapour no-saturation one. The black points are the OMEGA observations, the red one where the ice is found. The cyan curve is mean annual evolution of water vapour (pr-micron) along all the longitudes at latitude of 15°S (fig. 1a) and 30°S (fig. 1b, 1c). The red curves are the mean annual evolution of minimum and maximum temperature (K).